TELKOMNIKA Telecommunication, Computing, Electronics and Control
Vol. 18, No. 2, April 2020, pp. 1001~1011
ISSN: 1693-6930, accredited First Grade by Kemenristekdikti, Decree No: 21/E/KPT/2018
DOI: 10.12928/TELKOMNIKA.v18i2.14303

PID controller for microsatellite yaw-axis attitude control system using ITAE method

Ajiboye A. T.[1], Popoola J. O.[2], Oniyide O.[3], Ayinla S. L.[4]
[1,2,4]Department of Computer Engineering, University of Ilorin, Nigeria
[3]Department of Electrical and Electronics Engineering, University of Ilorin, Nigeria

Article Info

Article history:

Received Oct 10, 2019
Revised Jan 18, 2020
Accepted Feb 10, 2020

Keywords:

ITAE
Microsatellite attitude
Performance parameters
PID controller,
Pre-filter

ABSTRACT

The need for effective design of satellite attitude control (SAC) subsystem for a microsatellite is imperative in order to guarantee both the quality and reliability of the data acquisition. A proportional-integral-derivative (PID) controller was proposed in this study because of its numerous advantages. The performance of PID controller can be greatly improved by adopting an integral time absolute error (ITAE) robust controller design approach. Since the system to be controlled is of the 4th order, it was approximated by its 2nd order version and then used for the controller design. Both the reduced and higher-order pre-filter transfer functions were designed and tested, in order to improve the system performance. As revealed by the results, three out of the four designed systems satisfy the design specifications; and the PD-controlled system without pre-filter transfer function was recommended out of the three systems due to its structural simplicity, which eventually enhances its digital implementation.

Corresponding Author:

Ajiboye A. T.,
Department of Computer Engineering,
University of Ilorin, Ilorin, Nigeria.
Email: ajiboye.at@unilorin.edu.ng

1. INTRODUCTION

Satellites are exposed to many disturbances in space [1] which can adversely affect their attitude. The reliability of the microsatellite data acquisition is highly dependent on the quality of the SAC system because the attitude control system is crucial for accurate satellite operation [2]. Therefore, the needs for an accurate design of attitude control subsystem which guarantees the quality and reliability of the data. Several methods exist in the literature for achieving SAC. [3] and [4] proposed direct and modified adaptive controllers, respectively to mitigate different scenarios in spacecraft attitude control. Fixed-time [5], finite-time [6], adaptive gain based integral second order [7], fast terminal [8] and adaptive fast terminal [9] sliding mode techniques have been employed in rigid spacecraft attitude controller design.

Several applications of PID controller for satellite attitude control can be found in the literature. PID attitude controller for a rigid body satellite designed using a combination of Kharitonov theorem and vectored particle swarm optimization method was presented in [10]. Spacecraft control torque and velocity constraints dependent sliding mode based robust PID attitude controller were presented by Y. Li et al. [11]. Latest research by [12-16] employed an observer-based PID controller to control the attitude of a rigid satellite with ON/OFF thruster actuator which showed improvement in attitude control performance. The optimal PID controller for SAC, designed by [17] gave acceptable results for both the settling time and percentage overshoot, even though the bounds of controller parameters were arbitrarily

chosen [18] designed both PID and Fuzzy logic-based satellite attitude controllers in which the dynamics model of BILSAT-1 were utilized. Compared to the PID controller, the Fuzzy logic counterpart performed better in terms of system response speed and robustness. More so, [19] designed a PID controller to optimally control the satellite yaw attitude; and when tested via simulation, the settling time and percentage overshoot obtained were satisfactory as their values were within the design specifications.

PID controllers are popularly used in the control of industrial processes due to their structural and functional simplicity which in turn make their tuning relatively simple, most especially by a trial and error method [20]. It is also found in the majority of control systems due to its reliable performance and fine control capabilities [21]. At least 95% of control loops in process industries are PID in nature [22], which can be attributed partly to their robust performance in a wide range of operating conditions [23]. The performance of PID controller can be greatly improved by using an ITAE robust controller design which optimizes the controller gains, and subsequently the system performance parameters. The tool was adopted in this study as the system optimum performance parameters can be easily extracted as the system parameters and controller gains are varied [23]. Also, ITAE was identified as one of the best methods for robust control system designs [24]. The optimum coefficients for the ITAE performance criterion for a step input that can be used to find the best controller parameters have been determined for the standardized closed-loop transfer function in [23, 24]. Compared the results obtained by using Ziegler-Nichols and ITAE tuning methods for both first-order and second-order systems with dead time [25]. The results showed that ITAE tuning method was better than the Ziegler-Nichols tuning method in both scenarios. In most cases, the closed-loop response of the controlled system may not meet the desired specifications, under this condition a pre-filter transfer function must be designed and connected in series with the designed closed-loop system transfer function [24, 26]. It should be noted that all the parameters of the designed pre-filter transfer function are normally obtained directly from the dc gain and zeros of the designed closed-loop system transfer function [26].

2. DESIGN SPECIFICATIONS

The system design specifications considering unit step input are shown in Table 1. In this study, the system PO is a function of system damping ratio, while T_s is the time for which the system response remains within 2% of the final value as given in (1) and (2), respectively.

Table 1. Design specifications

Parameters	Values
Percentage Overshoot (PO)	≤ 5%
Settling time, T_s (for 2% criterion)	≤ 2 s
Steady-state error	0

$$P_o = 100e^{-\left(\zeta\pi/\sqrt{1-\zeta^2}\right)} \quad (1)$$

$$T_s = \frac{4}{\zeta\omega_n} \quad (2)$$

Where ζ and ω_n are the damping ratio and natural frequency in rad/sec for the closed-loop system. From (1):

$$\zeta = \frac{X^2}{\sqrt{(\pi^2 + X^2)}} \quad (3)$$

where $X = -\log 0.01PO$. Also, from (2),

$$\omega_n = \frac{4}{T_s\zeta} \quad (4)$$

in order to achieve the system design specifications, the threshold values for ζ and ω_n were determined using (3) and (4) [27]. The required conditions are $\zeta \geq 0.7797$ (≈0.8) and $\omega_n \geq 6$ rad/s.

3. SYSTEM MODEL

The yaw-axis attitude model for the satellite used in this study was derived based on a single input single output and linear time-invariant assumption which then yielded the transfer function that was used for the controller design.

3.1. Determination of open-loop transfer function and PID control algorithm selection

The yaw-axis ACS is represented by the block diagram of Figure 1 while its sub-systems' transfer functions are as expressed in (5)-(8).

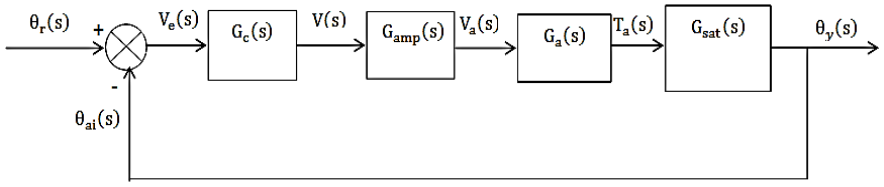

Figure 1. Block Diagram of microsatellite yaw-axis ACS

$$\mathrm{G_{sat}(s)} = \frac{\theta_y(s)}{T_a(s)} = \frac{1}{0.8s^2} \tag{5}$$

$$\mathrm{G_a(s)} = \frac{T_a(s)}{V_a(s)} = \frac{78.3s}{s^2 + 1815.4s + 24466} \tag{6}$$

$$\mathrm{G_{amp}(s)} = \frac{V_a(s)}{V(s)} = \frac{240}{0.1s + 1} \tag{7}$$

$$\mathrm{G_c(s)} = \frac{\mathrm{V(s)}}{V_e(s)} = \frac{K_D s^2 + K_P s + K_I}{s} \tag{8}$$

Where all the parameters are in Laplace Transform (s-domain); θ_y is the actual yaw attitude in degrees; T_a is the actuator torque in Nm; V_a is the motor armature voltage in volts; V is the controller output voltage in volts; V_e is error voltage in volts; $\mathrm{G_{sat}}$ is the satellite structure dynamic transfer function; $\mathrm{G_a(s)}$ is the actuator dynamic transfer function; $\mathrm{G_{amp}(s)}$ is the amplifier transfer function; $\mathrm{G_c(s)}$ is the controller transfer function; K_p is the proportional gain; K_i is the integral gain; and K_d is the derivative gain. The system open-loop transfer function shown in (9) was determined by cascading the transfer function of (5) to (8). The closed-loop transfer function obtained from (9) is as expressed in (10).

$$\frac{\theta_y(s)}{V_e(s)} = \frac{234900 * K_d s^2 + 234900 * K_p s + 234900 * K_i}{\mathrm{s^5 + 1825s^4 + 42625s^3 + 244625s^2}} \tag{9}$$

$$\frac{\theta_y(s)}{\theta_r(s)} = \frac{234900 * K_d s^2 + 234900 * K_p s + 234900 * K_i}{\mathrm{s^5 + 1825 * s^4 + 42625 * s^3 + (244625 + 234900 * K_d) * s^2 + 234900 * K_p s + 234900 * K_i}} \tag{10}$$

3.2. Reduction of system transfer function for controller design

An analysis of the uncontrolled system response to a specified test signal is necessary to determine the degree of the control effort required if any. To achieve this, the uncontrolled yaw-axis ACS open and closed-loop transfer functions, (11) and (12), were obtained from (9) and (10) respectively, assuming a unity controller transfer function. (12) was subjected to unit step function input and the resulting system step response is as shown in Figure 2. As shown in the Figure, the response will reach the set point at infinite time, therefore there is no overshoot, and settling time was 3.49 seconds. Considering this step response there is the need to incorporate a controller into the system so that the system design specifications shown in Table 1 can be achieved.

$$\frac{\theta_y(s)}{V(s)} = \frac{234900}{\mathrm{s^4 + 1825s^3 + 42625s^2 + 244625s}} \tag{11}$$

$$\frac{\theta_y(s)}{\theta_r(s)} = \frac{234900}{\mathrm{s^4 + 1825s^3 + 42625s^2 + 244625s + 234900}} \tag{12}$$

The PID control algorithm was considered due to its numerous advantages, such as simple design methodology and effectiveness in system control. It should be noted that PID control algorithm (either in full PID, PI or PD) performs better when the order of the system to be controlled is first, second or higher-order that can be approximated by either first or second-order dynamic [23]. The system to be controlled was reduced from 4th to a 2nd order using Balred reduction model, and the transfer function of the reduced-order version is as shown in (13). Both the 4th order and 2nd order versions exhibit good conformity, as evidenced in the plots of unit step responses of (12) and (13) shown in Figure 3.

$$G_{rcl}(s) = \frac{-0.16728s + 6.081}{s^2 + 6.002\,s + 6.096} \quad (13)$$

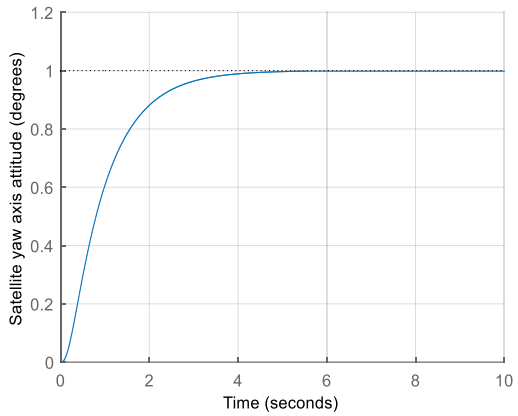

Figure 2. Uncontrolled closed-loop yaw-axis attitude step response

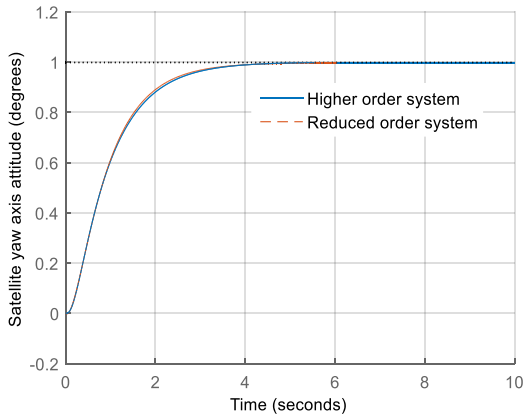

Figure 3. Plots of closed-loop unit step responses of the 4th and 2nd order of the uncontrolled system

The step response parameters of the two systems shown in Table 2 were obtained from Figure 3. Considering the closeness of the values, the higher-order one can be approximated by its reduced order version, which is subsequently used for PID controller design to achieve better performance.

Table 2. Step response parameters for uncontrolled higher and reduced-order closed-loop systems

Time-domain parameters	Higher-order system	Reduced-order system
Rise time (sec.)	1.890	1.800
Settling time (sec.)	3.490	3.290
Peak amplitude	0.998	0.997
Peak time (sec.)	5.230	5.580
% Overshoot	0.000	0.000
Steady state final value	1.000	0.998

$$G_{rcl}(s) = \frac{G_{rol}(s)}{1 + G_{rol}(s)} \quad (14)$$

Substituting (13) into (14) yields the open-loop transfer function of the reduced-order system $G_{rol}(s)$, as follows:

$$G_{rol}(s) = \frac{-0.16728s + 6.081}{\mathrm{s}^2 + 6.1693\mathrm{s} + 0.0150} \quad (15)$$

$$G_{rol}(s) = \frac{As + \mathrm{B}}{\mathrm{s}^2 + \mathrm{C}\,\mathrm{s} + \mathrm{D}} \quad (16)$$

where A = -0.1673, B = 6.081, C = 6.1693 and D = 0.0150.

4. CONTROLLER DESIGN

4.1. Determination of PID controller gains

The full PID controller transfer function is as expressed in (8), while the open-loop PID controlled transfer function for the reduced-order system was obtained by multiplying (8) and (16) to yield (17).

$$G_{rcol}(s) = \left(\frac{AK_d s^3 + (BK_d + AK_p)s^2 + (BK_p + AK_i)s + BK_i}{\mathrm{s}^3 + \mathrm{C}\mathrm{s}^2 + \mathrm{D}\mathrm{s}}\right) \quad (17)$$

Using (17) the closed-loop transfer function for the reduced-order PID controlled system, $G_{rccl}(s)$ is given by (18).

$$G_{rccl}(s) = \left(\frac{\left(\frac{1}{1+AK_d}\right)(AK_d s^3 + (BK_d + AK_p)s^2 + (BK_p + AK_i)s + BK_i)}{\mathrm{s}^3 + \left(\frac{BK_d + AK_p + \mathrm{C}}{1+AK_d}\right)\mathrm{s}^2 + \left(\frac{BK_p + AK_i + \mathrm{D}}{1+AK_d}\right)\mathrm{s} + \frac{BK_i}{1+AK_d}}\right) \quad (18)$$

The characteristic of (18) is (19).

$$\mathrm{s}^3 + \left(\frac{BK_d + AK_p + \mathrm{C}}{1+AK_d}\right)\mathrm{s}^2 + \left(\frac{BK_p + AK_i + \mathrm{D}}{1+AK_d}\right)\mathrm{s} + \frac{BK_i}{1+AK_d} = 0 \quad (19)$$

Since the characteristic equation of the transfer function is of 3rd order, the value of controller gains using ITAE design method can be determined by obtaining a standardised form of 3rd order characteristic equation. These can be found in the table of optimum coefficients of system closed-loop transfer function based on the ITAE criterion for a step input [23]. The obtained standardised characteristic equation from the table is given in (20).

$$\mathrm{s}^3 + 1.75\omega_\mathrm{n}\mathrm{s}^2 + 2.15{\omega_\mathrm{n}}^2\mathrm{s} + {\omega_\mathrm{n}}^3 = 0 \quad (20)$$

Where ω_n= 6 rad/s from (4). Equating the coefficients of s^3, s^2 and s in (19) and (20), and then rearranging, we can obtain

$$-0.1673K_p + 7.8377K_d = 4.3307 \quad (21)$$

$$6.081K_p - 0.1673K_i + 13K_d = 77.385 \quad (22)$$

$$K_i + 5.9426K_d = 35.5205 \quad (23)$$

The values of K_p, K_i and K_d are 11.8492, 30.7337, and 0.8055 respectively, obtained by solving (21), (22) and (23) simultaneously. The transfer function G_{rccl} of the closed-loop PID-controlled reduced-order system was obtained by substituting the values of A, B, C, D, $\mathrm{K_p}$, $\mathrm{K_i}$ and $\mathrm{K_d}$ in (18).

$$G_{rccl} = \frac{-0.1557\mathrm{s}^3 + 3.37\mathrm{s}^2 + 77.33\mathrm{s} + 216}{\mathrm{s}^3 + 10.5\mathrm{s}^2 + 77.35\mathrm{s} + 216} \quad (24)$$

Also, the transfer function G_{hccl} of the higher-order system of the PID was obtained by substituting the values of K_p, K_i and K_d in (10).

$$G_{\mathrm{hccl}} = \frac{189200(\mathrm{s}^2 + 14.71\mathrm{s} + 38.16)}{\mathrm{s}^5 + 1825\mathrm{s}^4 + 42625\mathrm{s}^3 + 433800\mathrm{s}^2 + 2783000s + 7219000} \quad (25)$$

4.2. Determination of PD controller gains

The uncontrolled system reduced-order open-loop transfer function was already given in (16). The PD controller transfer function was obtained from (8) by assuming $K_i = 0$ and is as expressed in (26).

$$G_c = (K_d s + K_p) \quad (26)$$

The open and closed-loop PD controlled reduced-order system transfer function were derived based on (16) and (26), as shown in (27) and (28) respectively.

$$G_{rcol} = \frac{(AK_d s^2 + (BK_d + AK_p)s + BK_p)}{\mathrm{s}^2 + \mathrm{Cs} + \mathrm{D}} \quad (27)$$

$$G_{rccl} = \frac{\left(\frac{1}{1 + AK_d}\right)(AK_d s^2 + (BK_d + AK_p)s + BK_p)}{\mathrm{s}^2 + \left(\frac{BK_d + AK_p + \mathrm{C}}{1 + AK_d}\right)\mathrm{s} + \frac{BK_p + \mathrm{D}}{1 + AK_d}} \quad (28)$$

The characteristic (28) is as shown in (29).

$$\mathrm{s}^2 + \left(\frac{BK_d + AK_p + \mathrm{C}}{1 + AK_d}\right)\mathrm{s} + \frac{BK_p + \mathrm{D}}{1 + AK_d} \quad (29)$$

The characteristic of (29) is of order 2, therefore to determine the PD controller gains values by applying ITAE method the corresponding standardised second-order characteristic equation was obtained from the optimum coefficients' table. The obtained characteristic equation is:

$$\mathrm{s}^2 + 1.4\omega_{\mathrm{n}}\mathrm{s} + {\omega_{\mathrm{n}}}^2 \quad (30)$$

where ω_{n}= 6 rad/s. Equating the coefficients of s^2 and s in (29) to (30) and rearranging, we have

$$-0.1673K_p + 7.4863K_d = 2.2307 \quad (31)$$

$$6.081K_p + -6.0228K_d = 35.9850 \quad (32)$$

the values of K_p and K_d were obtained as 5.5008 and 0.4209, respectively, by solving (31) and (32) simultaneously. Substituting the values of A, B, C, D, $\mathrm{K_p}$ and $\mathrm{K_d}$ in (28) gives (33).

$$G_{rccl} = \frac{0.07575(-\mathrm{s}^2 + 23.27\mathrm{s} + 475)}{(\mathrm{s}^2 + 8.4\,\mathrm{s} + 36)} \quad (33)$$

Substituting the values of K_p, K_d with K_i=0 into (10) gives the closed-loop transfer function of PD controlled higher-order system of (34)

$$G_{\mathrm{hccl}} = \frac{98870(\mathrm{s} + 13.07)}{\mathrm{s}^4 + 1825\mathrm{s}^3 + 42625\mathrm{s}^2 + 343500s + 1292000} \quad (34)$$

5. DESIGN OF PRE-FILTER TRANSFER FUNCTION

As can be seen from (24), (25), (33) and (34) both the reduced and higher-order PID and PD controlled closed-loop systems have zeros, which will negatively affect their response [23, 24, 26]. To ameliorate this effect, there is the need to incorporate pre-filter transfer function in series with the system closed-loop transfer function as shown in Figure 4. This is necessary to ensure that the resulting closed-loop transfer function will contain no zero and still maintain unity dc gain which will lead to the overall improvement of the system response [23]. Two pre-filter transfer functions were designed, the first

was based on the reduced-order system and the second was based on the higher-order system for each of the controller design.

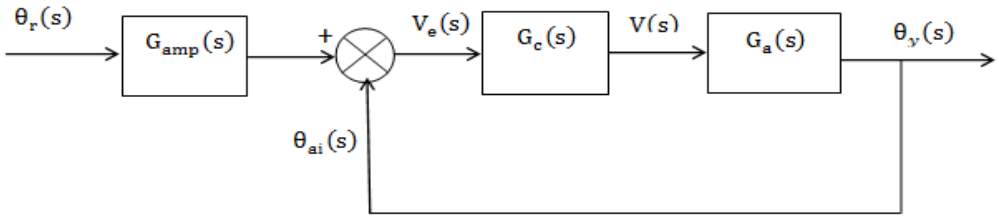

Figure 4. System closed-loop transfer function with pre-filter

5.1. Determination of pre-filter transfer function using PID controlled reduced-order system

Factorizing the numerator of (24) yielded (35).

$$G_{rccl} = \frac{0.1557(s - 36..3250)(s + 11.3653)(s + 3.3596)}{s^3 + 10.5s^2 + 77.35s + 216} \quad (35)$$

It can be seen from (35) that the introduction of PID controller transfer function into the system has added 2 more zeros to this system at $s = -11.3653$ and $s = -3.3596$ in addition to the already existing zero for the uncontrolled system which is at the point $s = 36.3250$. The expected closed-loop reduced-order PID controlled system transfer function when the pre-filter transfer function is introduced is as given in (36).

$$G_{rcclf} = \frac{216}{s^3 + 10.5s^2 + 77.35s + 216} \quad (36)$$

But,

$$G_{rcclf} = G_{rccl}G_{rf} \quad (37)$$

therefore, the lower order-based pre-filter transfer function (G_{rf}) was realized using (37) and is as expressed as

$$G_{rf} = \frac{1387}{(-s^3 + 21.6s^2 + 496.7s + 1387)} \quad (38)$$

As can be seen from (38), one of the poles of the reduced-order pre-filter transfer function is on the right-hand side of s-plane, therefore combining it in series with the controlled system closed-loop transfer function will cause instability. As a result, the response of the closed-loop controlled system with pre-filter will be different from the expected response of (36). In order to improve the system response, obtaining the pre-filter transfer function from the closed-loop PID controlled transfer function for the original higher-order system was considered.

5.2. Determination of pre-filter transfer function using higher-order PID controlled system

The PID controlled closed-loop transfer function for the original higher-order system is as shown in (25). Factorizing the numerator of (25) yielded (39), which shows that incorporation of PID controller into the system has increased the number of system zero from 0 to 2 and these zeros are at $s = -11.3470$ and $s = -3.3630$.

$$G_{\text{hccl}} = \frac{189200(s + 11.3470)(s + 3.3630)}{s^5 + 1825s^4 + 42625s^3 + 433800s^2 + 2783000s + 7219000} \quad (39)$$

Now the transfer function for the controlled closed-loop system with a pre-filter transfer function (G_{hcclf}) is as expressed in (40).

$$G_{\text{hcclf}} = G_{hf}G_{\text{hccl}} \quad (40)$$

Where: $G_{\mathrm{h}f}$ is the pre-filter transfer function obtained from the original higher-order control system. The expected controlled system transfer function with pre-filter is as expressed in (41).

$$G_{\mathrm{hcclf}} = \frac{7219000}{\mathrm{s}^5 + 1825\mathrm{s}^4 + 42625\mathrm{s}^3 + 433800\mathrm{s}^2 + 2.783000s + 7219000} \tag{41}$$

Therefore, from (39), (40), and (41),

$$G_{\mathrm{h}f} = \frac{38.16}{(\mathrm{s}^2 + 14.71\mathrm{s} + 38.16)} \tag{42}$$

Since $G_{\mathrm{h}f}$ is stable and can be used to improve the system response, therefore the transfer function for PID controlled higher-order system with higher-order pre-filter using (40) can be expressed as

$$G_{\mathrm{hcclf}} = \left(\frac{38.16}{\mathrm{s}^2 + 14.71\mathrm{s} + 38.16}\right)\left(\frac{189200(\mathrm{s}^2 + 14.71\mathrm{s} + 38.16)}{\mathrm{s}^5 + 1825\mathrm{s}^4 + 42625\mathrm{s}^3 + 433800\mathrm{s}^2 + 2783000s + 7219000}\right) \tag{43}$$

5.3. Determination of pre-filter transfer function from reduced-order PD controlled system

The PD controlled reduced-order closed-loop system transfer function is as shown in (33), which may be rewritten as,

$$G_{rccl} = \frac{0.07575(\mathrm{s} - 36.3407)(\mathrm{s} + 13.0707)}{(\mathrm{s}^2 + 8.4\,\mathrm{s} + 36)} \tag{44}$$

This shows that the introduction of PD controller into the system has increased the number of reduced-order system closed-loop zeros from 1, for the uncontrolled system located at $\mathrm{s} = 36.3522$ to 2 for the controlled system at $\mathrm{s} = 36.3522$ and $\mathrm{s} = -13.0707$. The expected closed-loop reduced-order PD controlled system with pre-filtered transfer function is as given in (45).

$$G_{rcclf} = \frac{36}{\mathrm{s}^2 + 8.4\,\mathrm{s} + 36} \tag{45}$$

But from (37),

$$G_{rf} = \frac{G_{rccl}}{G_{rcclf}} \tag{46}$$

therefore,

$$G_{rf} = \frac{475.2475}{(-\mathrm{s}^2 + 23.27\mathrm{s} + 475)} \tag{47}$$

The closed-loop reduced-order PD controlled system with this pre-filter transfer function will not give the expected pre-filtered closed-loop response because of the introduction of the right-hand side pole into the system by the pre-filter transfer function. Since the pre-filter transfer function obtained from the closed-loop reduced-order PD controlled system will destabilize the system, the next option is to obtain the pre-filter transfer function from the closed-loop PD controlled transfer function for the original higher-order system.

5.4. Determination of pre-filter transfer function from higher-order PD controlled system

The PD controlled closed-loop transfer function for the original higher-order system is as shown in (34). Factorizing the numerator of (34) gives (48).

$$G_{\mathrm{hccl}} = \frac{98870(\mathrm{s} + 13.07)}{\mathrm{s}^4 + 1825\mathrm{s}^3 + 42625\mathrm{s}^2 + 343500s + 1292000} \tag{48}$$

It can be seen from (48) that the introduction of PD controller into the system has increased the number of reduced-order system closed-loop zero from 0 for the uncontrolled system to 1 for the controlled system at

$s = -13.0707$. The expected PD controlled closed-loop transfer function for the original higher-order system with pre-filter transfer function is as shown in (49).

$$G_{\text{hcclf}} = \frac{1292000}{s^4 + 1825s^3 + 42625s^2 + 343500s + 1292000} \tag{49}$$

But from (40),

$$G_{\text{hf}} = \frac{G_{\text{hccl}}}{G_{\text{hcclf}}} \tag{50}$$

therefore,

$$G_{\text{hf}} = \frac{13.07}{(s + 13.07)} \tag{51}$$

From (51), the transfer function for PD controlled higher-order system with higher-order pre-filter is expressed as,

$$G_{\text{hcclf}} = \left(\frac{13.07}{s + 13.07}\right)\left(\frac{98870(s + 13.07)}{s^4 + 1825s^3 + 42625s^2 + 343500s + 1292000}\right) \tag{52}$$

6. SIMULATION

The controller design carried out in this paper has resulted into four types of controlled systems, namely PID controlled system without pre-filter, PID controlled system with pre-filter, PD controlled system without pre-filter and PD controlled system with pre-filter. It should be noted that the system of interest is the higher-order system which is the original system. Therefore, to select the most appropriate out of these four designed micro-SAC systems, there is the need to investigate their performance via simulation. Therefore, the system unit step response was plotted for these systems and the time domain performance parameters were extracted and used as the basis for selecting the most appropriate system after comparison. The time-domain performance parameters of interest are the rise time (T_r), settling time (T_s), percentage overshoot (PO), time to peak overshoot (T_p) and steady-state error (E_{ss}). To easy the system performance, comparison and analysis the system simulation was carried out using the uncontrolled and controlled systems closed-loop transfer functions as follows. Using (12), (25), (34), (43) and (52), the closed-loop step responses for the uncontrolled higher-order system; PID controlled higher-order system without pre-filter; PD controlled higher-order system without pre-filter; PID controlled higher-order system with pre-filter and PD controlled higher-order system with pre-filter were plotted as shown in Figure 5.

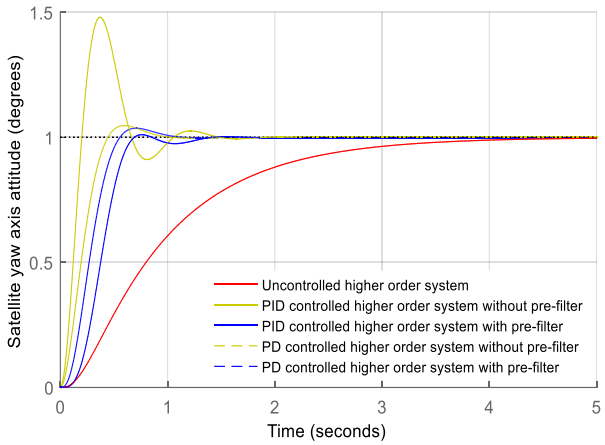

Figure 5. Closed-loop step response for uncontrolled and controlled higher order system

7. RESULTS AND DISCUSSION

The step response parameters in Table 3 were obtained from the uncontrolled and controlled systems closed-loop step response of Figure 5. As can be seen from Figure 5 and Table 3, the PID-controlled system without pre-filter has a better performance compared to the uncontrolled system when the rise time, settling time and time to peak overshoot were considered, but the performance becomes worse in terms of percentage overshoot. Introduction of pre-filter into the PID controlled system reduces the settling time and percentage overshoot but worsen both the rise time and time-to-peak overshoot by increasing the numerical value of these parameters. Introduction of pre-filter into the PD controlled system worsen the system performance by increasing the numerical value of the rise time, settling time and time to peak overshoot. But there is a reduction in the value of the percentage overshoot encountered by this system when compared to PD controlled system without pre-filter. Both the PD controlled systems without and with pre-filter have better performance compared to the uncontrolled system considering the rise time, settling time and time to peak overshoot. But the percentage overshoot for the uncontrolled system is less than that for any of the two PD controlled system.

Table 3. Step response performance parameters for yaw-axis attitude closed-loop controlled system

System condition	T_r (s)	T_s (s)	PO	T_p (s)	E_{ss}
Uncontrolled system	1.89	3.49	0	5.23	0
PID controlled system without pre-filter	0.136	1.31	48.1	0.37	0
PID controlled system with pre-filter	0.365	1.17	1.07	0.761	0
PD controlled system without pre-filter	0.288	0.814	4.73	0.593	0
PD controlled system with pre-filter	0.332	0.887	3.66	0.706	0

From the results, there are three major time-domain performance specifications to be satisfied; it can be seen in Table 3 that the uncontrolled system satisfies the PO and E_{ss} conditions, PID controlled system without pre-filter satisfied the T_s and E_{ss} conditions, PID controlled system with pre-filter satisfied the T_s, PO and E_{ss} conditions, the PD controlled system either with or without pre-filter satisfies the T_s, PO and E_{ss} conditions. Finally, three out of the four controlled systems designed satisfy the design specifications of $T_s \leq 2$ s, $PO \leq 5\%$, and $E_{ss} = 0$. It is noted that the three are the PID controlled system with pre-filter, PD controlled system without pre-filter and PD controlled system with pre-filter. Based on this analysis any of the three systems can be used but PD controlled system without pre-filter is the most preferable due to its structural simplicity which will enhance its digital implementation.

8. CONCLUSION

PID and PD controller-based microsatellite attitude controllers were designed. Pre-filter transfer functions were designed and incorporated into the designed systems to improve their performance. The designed systems were tested via simulation and the results revealed that three out of the four systems satisfy the design specifications and the PD controlled system without pre-filter transfer function is the most preferable due to its structural simplicity which will enhance its digital implementation.

REFERENCES

[1] B. Bohari, M. Ismail, R. Varatharajoo, and L. Nadia, "Spacecraft pitch and roll/yaw actuations using control moment gyroscopes for attitude stabilization," *Jurnal Mekanikal,* vol. 23, no. 23, pp. 1-14, 2017.
[2] X. Yi and A. Anvar, "Small-satellite magnetorquer attitude control system modelling and simulation," *20th International Congress on Modelling and Simulation*, Adelaide, Australia, pp. 984-990, 2013.
[3] J-F. Shi, S. Ulrich, and A. Allen, "Editors. Spacecraft adaptive attitude control with application to space station free-flyer robotic capture," *AIAA Guidance, Navigation, and Control Conference*, Florida, pp. 1-23, 2015.
[4] S. Sheng and C. Sun, "An adaptive attitude tracking control approach for an unmanned helicopter with parametric uncertainties and measurement noises," *International Journal of Control, Automation and Systems,* vol. 14, no. 1, pp. 217-228, 2016.
[5] B. Jiang, Q. Hu, and M. I. Friswell, "Fixed-time attitude control for rigid spacecraft with actuator saturation and faults," *IEEE Transactions on Control Systems Technology*, vol. 24, no. 5, pp. 1892-1898, 2016.
[6] P. M. Tiwari, S. Janardhanan, and M. un-Nabi, "Rigid spacecraft attitude tracking using finite time sliding mode control," *IFAC Proceedings Volumes,* vol. 47, no. 1, pp. 263-270, 2014.
[7] P. M. Tiwari, S. Janardhanan, and M. un-Nabi, "Rigid spacecraft attitude control using adaptive integral second order sliding mode," *Aerospace Science and Technology,* vol. 42, pp. 50-57, 2015.

[8] K. Lu, Y. Xia, M. Fu, and C. Yu, "Adaptive finite-time attitude stabilization for rigid spacecraft with actuator faults and saturation constraints," *International Journal of Robust and Nonlinear Control*, vol. 26, no. 1, pp. 28-46, 2016.
[9] K. Lu, Y. Xia, C. Yu, and H. Liu, "Finite-time tracking control of rigid spacecraft under actuator saturations and faults," *IEEE Transactions on Automation Science and Engineering,* vol. 13, no. 1, pp. 368-381, 2015.
[10] S. S. Kumar, C. Shreesha, and N. K. Philip, "Robust PID controller design for rigid uncertain spacecraft using Kharitonov theorem and vectored particle swarm optimization," *International Journal of Engineering and Technology (UAE)*, vol. 7, no. 2, pp. 9-14, 2018.
[11] Y. Li, S. Zhaowei, and Y. Dong, "Time efficient robust PID plus controller for satellite attitude stabilization control considering angular velocity and control torque constraint," *Journal of Aerospace Engineering*, vol. 30, no. 5, 2017.
[12] Y. Li, Z. Sun, and D. Ye, "Robust linear PID controller for satellite attitude stabilisation and attitude tracking control," *International Journal of Space Science and Engineering,* vol. 4, no. 1, pp. 64-75, 2016.
[13] Show L. L, Juang J. C, Lin C. T, and Jan Y. W, "Spacecraft robust attitude tracking design: PID control approach," *Proceedings of the 2002 American Control Conference*, USA, pp. 1360-1365, 2002.
[14] H. A. Hani, M. Y. Mashor, and M. C. Mahdi, "Performance of manual and auto-tuning PID controller for unstable plant-nano satellite attitude control system," *6th International Conference on Cyber and IT Service Management (CITSM)*, Medan, pp. 1-5, 2018.
[15] M. C. Mahdi, "Fuzzy PID controller for nano-satellite attitude control," *Journal of Science and Arts*, vol. 37, no. 4, pp. 407-416, 2016.
[16] V. Bohlouri, M. Ebrahimi, and S. H. Jalali-Naini, "Robust optimization of satellite attitude control system with on-off thruster under uncertainty," *International Conference on Mechanical, System and Control Engineering (ICMSC)*, pp. 328-332, 2017.
[17] S. K. H. Ar-Ramahi, "PID controller design for the satellite attitude control system," *Journal of Engineering,* vol. 15, no. 1, pp. 3312-3320, 2009.
[18] Adunola F. O., Sani S. M., and Dominic S. N., "Comparative study of FLC and PID for satellite attitude control," *Global Journal of Advanced Engineering Technologies*, vol. 5, no. 2, pp. 183-95, 2016.
[19] Mbaocha C. C., Eze C. U., Ezenugu I. A., and Onwumere J. C., "Satellite model for yaw-axis determination and control using PID compensator," *International Journal of Scientific & Engineering Research*, vol. 7, no. 7, pp. 1623-1629, 2016;
[20] F. A. Salem and A. A. Rashed, "PID controllers and algorithms: Selection and design techniques applied in mechatronics systems design-part II," *Int. J. of Engineering Sciences,* vol. 2, no. 5, pp. 191-203, 2013.
[21] P. Mohindru, G. Sharma, and P. Pooja, "Simulation performance of PID and fuzzy logic controller for higher order system," *Communications on Applied Electronics (CAE),* vol. 1, no. 7, pp. 31-35, 2015.
[22] K. J. Åström and T. Hägglund, "The future of PID control," *Control Engineering Practice*, vol. 9, no. 11, pp. 1163-1175, 2001.
[23] R. C. Dorf and R. H. Bishop, "Modern control systems," *Prentice Hall*, Pearson, New Jersey, 2010.
[24] A. O. Shuaib and M. M. Ahmed, "Robust PID control system design using ITAE performance index (DC motor model)," *International Journal of Innovative Research in Science, Engineering and Technology*, vol. 3, no. 8, pp. 15060-15067, 2014.
[25] F. G. Martins, "Tuning PID controllers using the ITAE criterion," *International Journal of Engineering Education*, vol. 21, no. 5, pp. 867-873, 2005.
[26] S. Zhang, Y. Tang, and C. Luo, "Analytical design of controller orienting higher-order closed-loop systems to minimum deadbeat response," *IOP Conference Series: Earth and Environmental Science*, vol. 69, pp. 1-7, 2017.
[27] E. A. Hussein and M. H. Waly, "Proportional-integral (PID) controller design using genetic algorithm (GA)," *Al-Qadisiyah Journal for Engineering S.*